

Rainfall-discharge Relationships for Monsoonal Climates

Authors

Tammo Steenhuis, Cornell University, USA

Joie Taylor, Decatur Healing Arts, USA

Amy Collick, Bahir Dar University Ethiopia

Nick van de Giesen, Delft University of Technology, The Netherlands

Jens Liebe, Center for Development Research, University of Bonn, Germany

Marc Andreini, International Water Management Institute, USA

Zach Easton, Cornell University, USA

Scope

Methods for estimating runoff that have been developed for temperate climates may not be suitable for use in the monsoonal climates of Africa, where there is a distinct dry season in which soils dry out to a considerable depth. This has a distinct effect on runoff generation that is not captured by “the temperate climate” models.

The scope of this tool is to develop a simple water balance method for predicting river discharge. Water balance models have been shown to better predict river discharge in regions with monsoonal climates than alternative methods based on the USDA-SCS curve number. The latter is an empirical based model developed in the USA that does not apply to monsoonal climates with distinct dry and wet periods

Target group

Hydrologists, water resources planners

Requirements for application

Precipitation data, evaporation data, information on watershed boundaries, a GIS system.

Description and application:

Doing a water balance for a watershed is simple! In many regions, rainfall intensity does not affect runoff, in which case we can simply take daily, weekly or even monthly precipitation amounts, subtract evaporation, and use the water balance to keep track of moisture content in the root zone. There is an upper limit for soil moisture (field capacity). When this is exceeded, water drains out of the profile either by percolation to groundwater, as interflow, or as surface runoff. Evaporation is dependent on soil moisture content. It is known that evaporation is zero at wilting point and approaches the potential rate when the soil is at field capacity. There is a linear relationship of evaporation and moisture content between these two points.

The watershed model has many similarities with a flowerpot. Water is added. Add too much water and it drains out. When the soil is dry the plant wilts and evaporation is reduced. A real

watershed may be conceived as being composed of many “flowerpots” of different sizes. For simplicity we assume only two areas: hill slopes, and the relatively flat areas that become saturated during the rainy season. Hill slopes have high percolation rates (McHugh, 2006) and water is generally transported subsurface as interflow (e.g. over a restrictive layer) or base flow (percolated from the profile). The flatter areas that drain the surrounding hill slopes become runoff source areas when saturated (Fig. 1 shows a schematic). The profile for the hill slopes is divided into a root zone where the plants extract water and a bottom layer that transmits excess water to the stream. In the saturated contributing area all excess water becomes surface runoff. As this is our major point of interest, we simulate only the top layer (root zone) in this application.

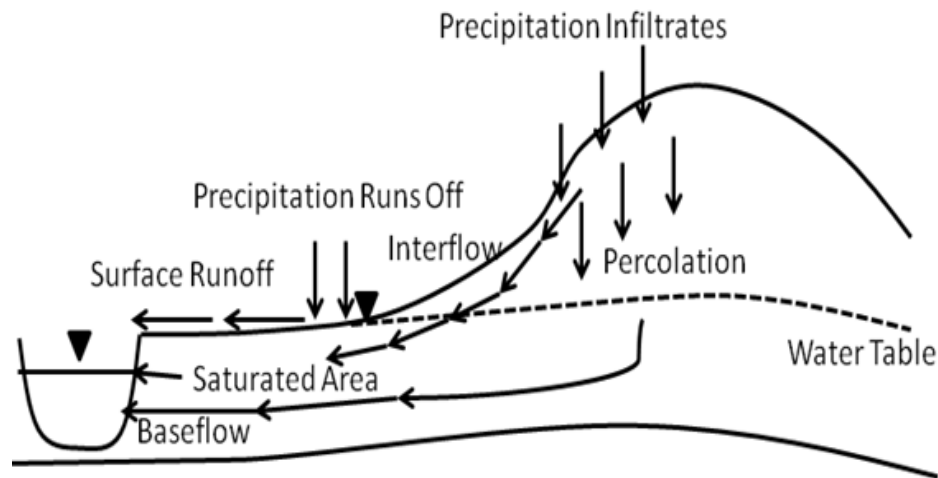


Figure 1: Schematic landscape segment

The amounts of water stored in the topmost layer of the soil, S (mm), for hillslopes and for runoff source areas, were estimated separately with a water balance equation of the form:

$$S = S_{t-\Delta t} + (P - AET - R - Perc)\Delta t \quad (1)$$

where P is precipitation, (mm d^{-1}); AET is the actual evapotranspiration; $S_{t-\Delta t}$, previous time step storage, (mm), R saturation excess runoff (mm d^{-1}), $Perc$ is percolation to the subsoil (mm d^{-1}) and Δt is the time step.

During wet periods, when rainfall exceeds evapotranspiration (i.e., $P > PET$), actual evaporation, AET , is equal to potential evaporation, PET . Conversely, when evaporation exceeds rainfall (i.e., $P < PET$), the Thornthwaite and Mather (1955) procedure is used to calculate actual evapotranspiration, AET (Steenhuis and van der Molen, 1986). In this method AET decreases linearly with moisture content, e.g.

$$AET = PET \left(\frac{S_t}{S_{\max}} \right) \quad (2)$$

where PET is potential evapotranspiration (mm d^{-1}). The available soil storage capacity, S_{max} , (mm) is defined as the difference between the amount of water stored in the top soil layer at wilting point and the upper moisture content that is equal to either the field capacity for the hillslopes soils or saturation in runoff contributing areas. S_{max} varies according to soil characteristics (e.g., porosity, bulk density) and soil layer depth. Based Eq. 2 the surface soil layer storage can be written as:

$$S_t = S_{t-\Delta t} \left[\exp \left(\frac{(P - PET)\Delta t}{S_{max}} \right) \right] \quad \text{when } P < PET \quad (3)$$

In this simplified model direct runoff occurs only from the runoff contributing area when the soil moisture balance indicates that the soil is saturated. The recharge and interflow comes from the remaining hill slopes areas. There is no surface runoff from these areas. This will underestimate the runoff during major rainfall events but since our interest in weekly to monthly intervals this is not thought to be a major limitation.

In the saturated runoff contributing areas, when rainfall exceeds evapotranspiration and fully saturates the soil, any moisture above saturation becomes runoff, and runoff, R , can be determined by adding the change in soil moisture from the previous time step to the difference between precipitation and actual evapotranspiration, e.g.,

$$R = S_{t-\Delta t} + (P - AET)\Delta t \quad (4a)$$

$$S_t = S_{max} \quad (4b)$$

In hill slopes, water flows either as interflow or baseflow to the stream. Rainfall in excess of field capacity becomes recharge and is routed to two reservoirs that produce baseflow or interflow. We assumed that the baseflow reservoir is filled first and when full the interflow reservoir starts filling. The baseflow reservoir acts as a linear reservoir and its outflow, BF_t , and storage, BS_t , are calculated when the storage is less than the maximum storage, BS_{max}

$$BS_t = BS_{t-\Delta t} + (Perc - BF_{t-\Delta t})\Delta t \quad (5a)$$

$$BF_t = \frac{BS_t [1 - \exp(-\alpha\Delta t)]}{\Delta t} \quad (5b)$$

When the maximum storage, BS_{max} , is reached then

$$BS_t = BS_{max} \quad (6a)$$

$$BF_t = \frac{BS_{max} [1 - \exp(-\alpha\Delta t)]}{\Delta t} \quad (6b)$$

Interflow originates from the hill slopes, and landscape slope is the major force driving water movement. Under these circumstances, the flow decreases linearly (i.e., a zero order reservoir)

after a recharge event. The total interflow, IF_t at time t can be obtained by superimposing the fluxes for the individual events (details are given in the Appendix):

$$IF_t = \sum_{\tau=0,1,2}^{\tau^*} 2Perc_{t-\tau}^* \left(\frac{1}{\tau^*} - \frac{\tau}{\tau^{*2}} \right) \quad (7)$$

where τ^* is the duration of the period after the rainstorm until the interflow ceases, IF_t is the interflow at a time t , $Perc_{t-\tau}^*$ is the remaining percolation on $t-\tau$ days after the base flow reservoir is filled. To demonstrate the method we give two examples: the Abay (Blue Nile) and the Volta.

Application: the Abay Blue Nile

For the Blue Nile we predicted the ten-day averaged river discharge at the El Karo gauge station at the Ethiopian-Sudan border for 1993-1994. The ten-day averaged precipitation over the entire Abay Blue Nile basin in Ethiopia is also available for this period (Ahmed 2003, Fig. 2). Other parameters needed to simulate the discharge include: potential evapotranspiration, which varies little between years and was set at 5 mm d^{-1} during the dry season and 3.3 mm d^{-1} during the rainy season, and soil parameters (e.g., storage). Values for soil storage for the hill slopes and the contributing area were based initially on values from Collick et al. (2008) for three SRCP watersheds. Although the Collick et al. (2008) values resulted in a reasonable fit in this application, we decided to vary them slightly to improve the agreement between observed and predicted values. (The correct distribution between subsurface flow and overland flow directly determines predicted sediment concentrations: Steenhuis et al, 2008). Maximum storage values S_{\max} , for different parts of the watershed are listed in Table 1.

Simulating the subsurface flow in the complex landscape of the Blue Nile required both a linear (first order) ground water reservoir to correctly predict the base flow at the end of the dry season and zero order reservoir to obtain the interflow from the hillslope. The best fit to observed streamflow data was obtained with reservoir coefficient α of 20 mm and a τ^* of 140 days.

Observed rainfall and predicted and observed discharge are shown in Fig. 2. The various components (i.e., direct runoff, and the sum of the interflow from hill slopes and baseflow) are shown in Fig. 3. At the beginning of the rainy season almost all flow in the river is direct runoff generated from the 20% of the area that has the smallest storage. As the rainy season progresses (cumulative rainfall increases), the rest of the landscape wets up and runoff is generated from the remaining 10% of the flatter contributing area, followed in early July 1993 by base and interflow from the hill slopes. Note that this corresponds to the time when sediment concentration in the river is decreasing from a maximum value (Fig. 4).

Less obvious but just as important is that the volumes of predicted and observed discharge in Fig. 2 (i.e., areas under the curves) are equal, indicating that the water balance does indeed balance within a hydrologic cycle. In other words we can account for all precipitation that does not evaporate as stream flow in the same year. Finally, this water balance is able to explain the observed runoff coefficient of (i.e., discharge/precipitation) of approximately 20-30% during

the period when most rainfall occurs by distributing the effective rainfall (rainfall minus potential evaporation) over saturated contributing areas that generate direct runoff - and then interflow and baseflow after the major rainfall from the remaining 70% of the area.

Table 1: Model inputs: fractional areas of watershed, S_{max} values, and type of area.

Fraction of Watershed	Storage S_{max} (mm)	Type
0.2	10	contributing area
0.1	250	contributing area
0.7	500	hillside

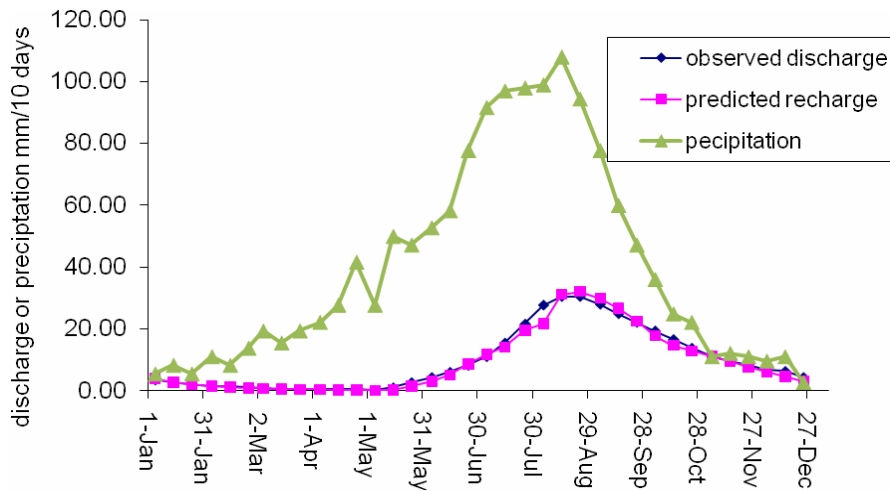


Figure 2: Ten day precipitation, and predicted and observed discharge for the Abay Blue Nile at El Karo, Sudan.

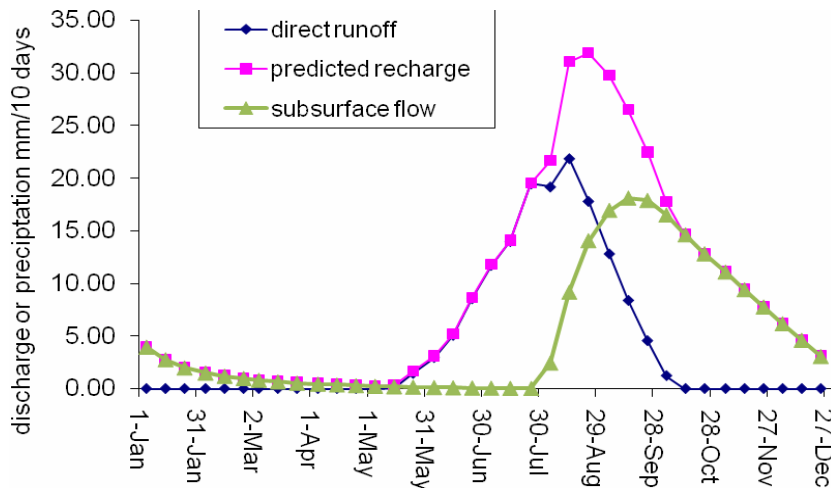


Figure 3: Predicted total discharge, direct runoff, and subsurface flow for the Abay Blue Nile at El Karo at the Ethiopian Sudanese Border

The Volta Basin

The Volta basin is much less steep than the Blue Nile basin. Although the same general principles govern water balance, practical implementation is different. In the relatively flat Volta basin, the fast and relatively rapid interflow along the hill slopes characteristic of the Blue Nile basin does not occur. This means that the zero order reservoir and the saturated areas can be neglected in Volta basin simulations and all stream flow is base flow from a linear reservoir recharged by the (relatively flat) hillside. Due to the flat slopes only a portion of the hillside areas contribute to stream flow. In the remaining area the water that percolates down to root zone is used by deep rooted vegetation during the dry season.

Precipitation data was derived from the Global Gridded Climatology (GGC) compiled by the Climatic Research Unit at a resolution of 0.50 lat/long, (New *et al.*, 1999a, b). The Climatic Research Unit (CRU) (New *et al.*, 1999a, b) also provided vapor pressure data, wind speed, and temperature, used to calculate *PET* using the Penman equation. Both precipitation and *PET* estimates were made by overlaying a map of the area on a grid. Each pixel, at $0.5^\circ \times 0.5^\circ$ per cell (1 cell $\approx 11,700 \text{ km}^2$), was weighted by that pixel's contribution to the total area, and the monthly mean was computed by adding the weighted pixels in the total area (Andreini *et al.*, 2000). To fit the predicted stream flow, two sources of stream discharge, obtained from WRI of Ghana and L'Institut de Recherche pour le Développement (ORSTOM), proved advantageous. Figure 4 shows the location of each streamflow gage. Table 2 contains the stations that had data of acceptable accuracy. Station accuracy was assessed by Taylor *et al* (2006).

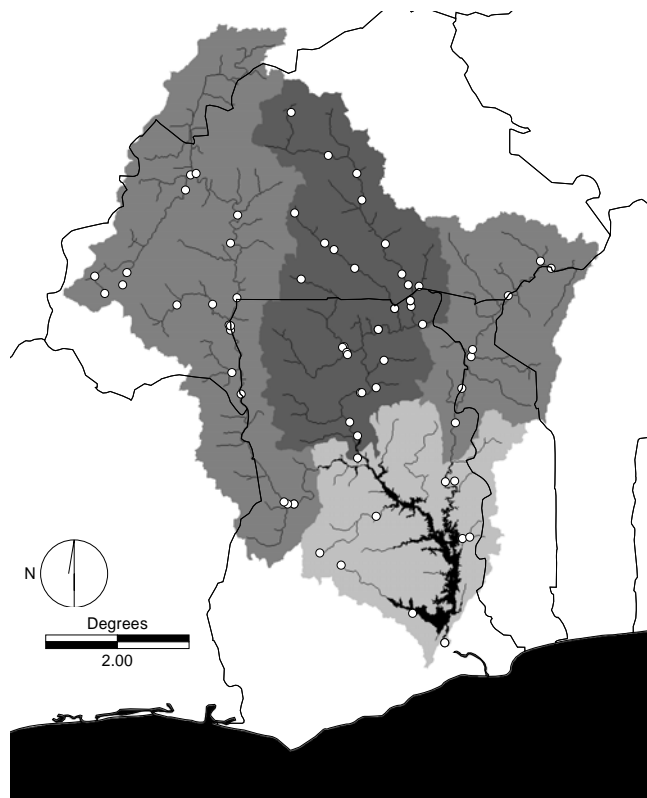


Figure 4: Stream flow gages in the Volta Basin

In Table 2, best fit parameter values for the water balance are all within reasonable values from the literature, and are consistent with results from prior work in the basin. Figure 5 shows the results of monthly predictions of river discharge. The r^2 values are 0.66 for WRI data and 0.56 for ORSTOM data. The S_{\max} values for the Black Volta Basin are 60 mm on average with a standard deviation of 29 mm. For the White Volta and the Oti, maximum available water contents are 112 mm and 143 mm, respectively, both with a standard deviation of 50 mm. The average available water content for the Lower Volta proper is 70 mm with the exception of Prang (the uppermost, wetter subcatchment), which has an available water content of 350 mm. These values are consistent with the parameters found in Dunne and Leopold (1978) for moderately deep-rooted crops (between 75 and 200 mm) and for clay in mature forest (above 350 mm).

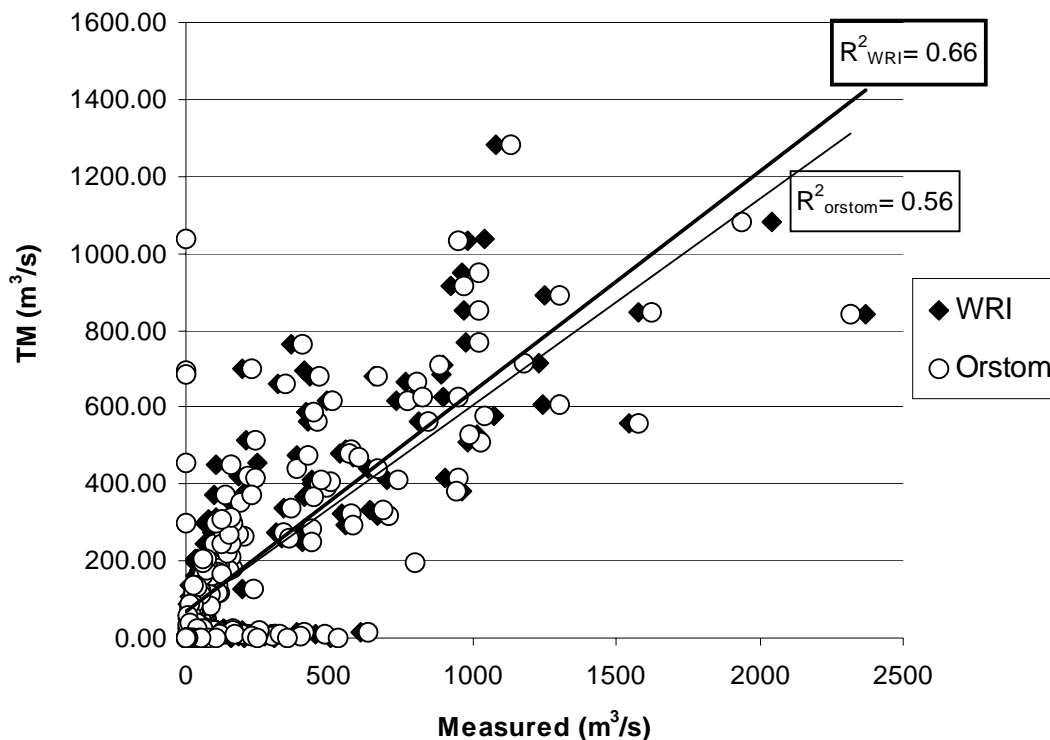


Figure 5: Results of monthly predictions of river discharge

The portions of available runoff that actually enter the stream (delivery ratio) for each month (the α parameter) in the White Volta, the Volta proper, and the Oti, 0.56, 0.48, and 0.48, respectively, are almost identical to the values used by Thornthwaite and Mather (Thornthwaite and Mather, 1955) for North Carolina, which, in many regards, has a similar topography as the Volta basin. Values for the Black Volta are consistently lower. The percent area of the watershed that contributes to runoff is typical for a semi-arid landscape. Average β values for the White Volta, and Oti are similar and higher than the Black Volta, which also has lower available water contents on average. As expected, the wetter the basin, the greater the contributing area.

Table 2: Parameter values for various gages in the Volta basin

Gage Name	S_{max} (mm)	1/month	%	R²	Years of record
Black Volta	60	0.35	35	0.60	18
Bamboi-W	83	0.33	58	0.66	25
Bamboi -O	83	0.33	58	0.56	30
Tainso (Tain)	84	0.50	11	0.56	13
Bui	39	0.35	58	0.63	35
Kalbuipe (Sur)	83	0.41	20	0.66	22
Dapola	33	0.31	30	0.61	10
Lawra-W	52	0.28	32	0.64	13
Lawra-O	52	0.28	32	0.60	11
Dan (Boug)	90	0.42	21	0.63	15
Diebouyou (B)	92	0.40	37	0.67	18
Ouessa	20	0.33	25	0.68	6
Banzo	74	0.44	48	0.70	40
Boromo	20	0.27	30	0.47	10
Tenado	24	0.30	41	0.55	11
Nwokuy	100	0.30	38	0.55	20
Manimenso	33	0.34	20	0.48	8
White Volta	112	0.56	63	0.68	37
Lankatere(Mo)	176	0.75	87	0.77	72
Nawuni-O	66	0.50	60	0.76	19
Nasia (Nasia)	163	0.55	64	0.82	33
Yagaba (Kalp)-O	109	0.61	68	0.77	58
Wiasi-O (Sisili)	86	0.62	43	0.72	23
Ngodi (Naz)-W	71	0.32	55	0.26	20
Oti	143	0.48	68	0.63	40
Ekumdipe (Da)	174	0.50	100	0.73	47
Sabari	167	0.40	80	0.80	31
Saboba	133	0.65	100	0.71	62
Koumangu (K)	200	0.61	100	0.86	90
Mango	161	0.35	94	0.68	42
Porga	101	0.35	47	0.70	23
Arly	27	0.30	16	0.53	6
Arly (Dou)	180	0.70	10	0.00	19
Volta Prop	139	0.48	52	0.55	65
Senchi (37-63)	70	0.33	69	0.72	26
Senchi (51-80)	63	0.55	59	0.37	43
Aframso (Afr)	67	0.37	50	0.53	6
Ahamnasu (A)	73	0.39	38	0.64	89
Podoe	67	0.45	18	0.34	12
Prang (Pru)	351	0.70	100	0.69	153

Lessons learned

The hydrological model presented here is based on a simple water balance method (dividing the watershed up into saturated areas that produce runoff and hill slope areas that recharge the aquifer). It was found to be reasonably robust. The relative portion of each area depends on the type of landscape and climate.

Recommendations

Only limited testing of this tool has taken place. Further testing should be conducted when more data becomes available. Data from the reservoirs are ideally suited for this purpose.

Limitations

The tool can only predict runoff volumes on a “per storm” storm basis. Finer scale predictions are limited because travel times are not considered. Moreover although runoff volume depends only on total rainfall, total flow during the storm also depends on rainfall intensity; thus runoff volume plotted as a function of both time and on intensity.

References

- Ahmed A.A., 2003. Sediment Transport and Watershed Management Blue Nile System, Friend/Nile Project report, Sudan.
- Andreini, M., N.C. van de Giesen, A. van Edig, M. Fosu, W. Andah, 2000. Volta Basin Water Balance; ZEF-Discussion Papers on Development Policy, Number 21. Bonn, Germany. Center for Development Research.
- Brutsaert, W., and Nieber J.L. 1977. Regionalized drought flow hydrographs from a mature glaciated plateau, *Water Resources. Research* 13, 637-643.
- Collick, A.S., Easton, Z.M., Adgo, E., Awulachew, S.B., Zeleke Gete, and Steenhuis, T S. 2008. Application of aphysically-based water balance model on four watersheds throughout the upper Nile basin in Ethiopia. In: Eds. W. Abteu and A. M. Melesse. *Proceedings of the 2008 workshop on the Nile Basin hydrology and ecology under extreme climatic conditions.*
- Conway D. 1997. A water balance model of the Upper Blue Nile in Ethiopia. *Hydrological Sciences Journal* 42(2): 265–286.
- Johnson P.A., Curtis P.D. 1994. Water-balance of Blue Nile river basin in Ethiopia. *Journal of Irrigation and Drainage Engineering-ASCE* 120(3):
- Kebede S, Travi, Y, Alemayehu T, Marc V. 2006. Water balance of Lake Tana and its sensitivity to fluctuations in rainfall, Blue Nile basin, Ethiopia. *Journal of Hydrology* 316: 233–247.
- Lui, B.M., A.S. Collick, G. Zeleke, E. Adgo, Z.M. Easton, and T.S. Steenhuis. 2008. Monsoonal rainfall-discharge relationships. *Hydrological Processes* 22.
- McHugh O.V. 2006. Integrated water resources assessment and management in a drought-prone watershed in the Ethiopian highlands. PhD dissertation, Department of Biological and Environmental Engineering. Cornell University Ithaca NY.
- New, M., M Hulme., and P. Jones (1999a). Representing twentieth century space-time variability. I: Development of a 1961-1990 mean monthly terrestrial climatology. *Journal of Climate* 12:829-856.
- New, M., M. Hulme, and P. Jones (1999b). Representing twentieth century space-time climate variability. II: Development of 1901-1996 monthly grids of terrestrial surface climate. *Journal of Climate* 13:2217-2238.
- Steenhuis, T.S., Collick, A.S. , Awulachew, S.B., Enyew Adgo, A., Abdassalam A., and Easton, Z.M. 2008. Modelling Erosion and Sedimentation in the Upper Blue Nile *In: Eds. W. Abteu and A. M.*

Melesse. Proceedings of the 2008 workshop on the Nile Basin hydrology and ecology under extreme climatic conditions.

Taylor J.C., van de Giesen N., Steenhuis T.S. 2006. West Africa: Volta discharge data quality assessment and use. *Journal of the American Water Resources Association* 42 (4): 1113-1126